

Model of Water and Solute Active Transport through the Epidermis: Role of the Keratinocytes

Cibele Vieira Falkenberg

Mechanical & Industrial Engineering Dept.
University of Illinois at Urbana-Champaign
falkenbe@uiuc.edu

John G. Georgiadis

Mechanical & Industrial Engineering Dept. and Bioengineering Dept.
University of Illinois at Urbana-Champaign
georgia@uiuc.edu

Abstract. Seeking to explain the performance of human skin as an effective transport barrier, this study focuses on active mass transport associated with epidermal cells (keratinocytes). We model the redistribution of water coupled to ion transport in a coarse-grained model of the skin consisting of free interstitial water, live cells, and inert extracellular matrix (active triphasic medium). The volume of the cell phase depends on the fluxes of water and Na^+ , K^+ and Cl^- ions across the cell membrane and is regulated according to the model of Hernandez and Cristina, 1998. A parametric numerical simulation study of the response of the active triphasic medium exposed to osmotic shocks at one boundary reveals novel travelling waves in the case of hyposmotic shocks.

keywords: epidermis, active transport, keratinocytes, triphasic medium

1. Introduction

The thermal and chemical barrier function of the skin is intimately connected to a combination of its structural characteristics and the exchange and redistribution of water and electrolytes in each one of its three layers, cf. Freinkel and Woodley, 2001. The epidermis, the outmost layer of the skin, consists of stratified squamous self-regenerating epithelial tissue without any blood vessels. Protected underneath the keratinized stratum corneum layer consisting of cells that are eventually sloughed off, the epidermis is made of viable cells, 90 % to 95 % of which are keratinocytes (Freinkel and Woodley, 2001), and extracellular matrix which is perfused by interstitial water. A basement membrane connects the dermis (the second layer) to the epidermis. It provides structural support, binding, controls epithelial growth and differentiation (barrier to downward growth). The basement membrane also acts as a selective barrier, regulating permeability and also permits flow of nutrients metabolites and other molecules, since no blood vessels go to the epidermis. The epidermis is the most important layer for mass transport for two reasons: First, combining both intracellular and extracellular water, the greatest water content difference is found there, from more than 70 % (on the basement membrane) to 15 % (on top of the stratum corneum). Second, the epidermis is totally non-vascular, while the two lower layers (dermis and hypodermis) are highly vascular and therefore introduce convective transport pathways which makes them extremely permeable. The skin appendages are embryonically derived from the surface epithelium, but are found in the hypodermis (hair, merocrine sweat glands) and in the dermis (sebaceous glands, erector pili). Of particular importance are the sweat ducts that provide tortuous paths for water from the sweat glands to the surface of the epidermis. We will ignore all skin appendages in this study, which eliminates the possibility of bulk water motion across the epidermis.

We assume that the epidermal barrier action can be decomposed into the passive contribution of the stratum corneum and the active component of the viable layer below, from the stratum corneum down to the basal membrane. Here, "active" does not refer to the overall property of the epidermis to transport species against their concentration gradient. This characterization pertains to the active transport across the individual epidermal cells. These cells are nourished by interstitial fluid (water and electrolytes) that comes from the perfused dermis below. The complex but passive contribution of the non-viable stratum corneum to the barrier function of the epidermis, cf. Freinkel and Woodley, 2001, is outside the scope of the present investigation. The emphasis of this study is on modelling the variation of interstitial (extracellular) water and the concentration of three physiologically-relevant ions (Na^+ , K^+ and Cl^- ions) through the viable non-swelling epidermis, by including active transmembrane transport through the keratinocytes. The controversies surrounding the mechanisms of

water transport notwithstanding, cf. Reuss and Hirst, 2002 and Chinard, 2000, we adopt a coarse-grained model for the cell volume regulation developed by Hernandez and Cristina, 1998. The question addressed here is whether the coupling between active (intracellular or trans-cellular) and diffusive (extracellular or para-cellular) mass transport introduces any atypical features. Since the ultimate goal of our study is to develop rational transepidermal transport models, any such features can help validate these models through experiments, cf. Verkman, 2000.

2. Methodology

This section focuses on the formulation of a coarse-grained model for water and ion transport through the composite medium consisting of the phases α , β and γ as depicted in Fig. 1. Phase α is modelled as a homogeneous aqueous medium consisting of water and dissolved ions. Since we have excluded the stratum corneum from our investigation, phase α simply accommodates the swelling of phase β . This aspect of our model makes different from other hydrated tissue models, cf. Gu et al., 1998; Gu et al., 1999. Of course, these models do not account for the active participation of one of the tissue constituents, like the cell phase introduced here. The cell volume regulation is dependent on the fluxes of Na^+ , K^+ and Cl^- ions across the cell membrane and the density of the $Na^+ - K^+ - ATPase$ membrane. The ion fluxes depend on the local interior and exterior ion concentrations. The phase β is modelled according to Hernandez and Cristina, 1998, where all these interactions are considered. Each cell is considered to have uniform internal concentration of all solutes and acts as a source or sink of solute and water to phase α . The phase γ , which is part of the extracellular environment, is rigid and inert (adiabatic) in terms of mass transport. We assume that only diffusive transport of Na^+ , K^+ and Cl^- ions and X , representing other solutes that do not cross the cell membrane, is taking place in phase α while the water is re-distributed between phases α and β according to the cell regulation model. We found that the effect of the electrostatic potential variation across the layer (electrodifussion) is negligible, cf. Falkenberg and Georgiadis, 2004. In the following, we formulate the water and solute exchange model for a triphasic model of the epidermis without net convective motion and perform a numerical simulation study of its behavior by exposing it to hyposmotic and hyperosmotic shocks of variable strength.

2.1. Formulation of Polyphasic Model

The structure of the epidermis can be simplified in terms of a composite model consisting of three basic domains: free extracellular water, α , intracellular space, β , and a third domain, γ , composed by fibers, keratin, other proteins and dead cells. This decomposition in three domains, or phases, allows a coarse-grained representation of the epidermis as far as water and solute exchange is concerned. The spatial characteristic scale in this representation becomes larger than the Representative Elementary Volume (REV) which is larger than the scale of a single epidermal cell, as indicated in Fig. 1. Overall, the α phase occupies a multiply-connected domain which is bounded by the basement membrane and the stratum corneum on the outer surface of the skin. The mathematical formulation is based on a generic model for porous media, as described by Bear and Buchlin, 1987.

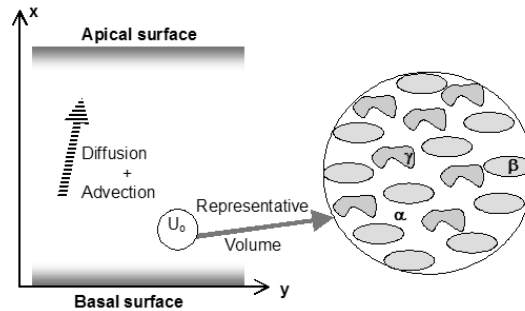


Figure 1: Schematic of the viable epidermal layer as a triphasic medium.

The model is formulated in terms of the standard volumetric superficial and phase averages of a given property, say e , which are denoted by $\langle e_{\alpha i} \rangle$ and $\langle e_{\alpha i} \rangle^{\alpha i}$, respectively, where αi denotes the phase. The ratio of the two averages defines the volumetric fraction $\theta_{\alpha i}$,

$$\langle e_{\alpha i} \rangle = \theta_{\alpha i} \langle e_{\alpha i} \rangle^{\alpha i} \quad (1)$$

It is assumed that no chemical transformation occurs so that the production rates are zero for all phases. Four

governing equations can be derived by equating e with the molar concentration c_i [mol/cm³] of each i component (such as the Na^+ , K^+ and Cl^- ions, and the generic solute X which does not cross the cell membrane).

$$\sum_{\alpha i} \frac{\partial (\theta_{\alpha i} \langle c_{i \alpha i} \rangle^{\alpha i})}{\partial t} = - \left(\sum_{\alpha i} \nabla \cdot (\theta_{\alpha i} \langle \mathbf{j}_{i \alpha i}^* \rangle^{\alpha i}) \right) - \left(\sum_{\alpha i} \nabla \cdot \langle c_{i \alpha i} \mathbf{v}_{\alpha i}^* \rangle \right) \quad \alpha i = \alpha, \beta, \gamma \quad (2)$$

The molar velocity averaged over all components is denoted by \mathbf{v}^* . The net diffusive flux can be modelled by using an effective transport coefficient $\mathbf{D}_{\mathbf{mi}}^*$ in the place of the molar diffusion coefficient $\mathbf{D}_{\mathbf{mi}}$.

$$\langle \mathbf{j}_{i \alpha i}^* \rangle^{\alpha i} \equiv -\mathbf{D}_{\mathbf{mi}}^* \cdot \nabla \langle \mathbf{c}_{i \alpha i} \rangle^{\alpha i} \quad (3)$$

In order to suppress some of the cumbersome notation, henceforth, transport coefficients pertain to the phase on which the corresponding gradient operator is defined. The assumptions that phase γ (connective tissue) does not participate and that there is no advection in β phase, allow the following simplifications of the coarse-grained model adopted here:

$$\frac{\partial \theta_\gamma}{\partial t} = 0 \quad (4)$$

$$\frac{\partial \langle c_{i \gamma} \rangle^\gamma}{\partial t} = \nabla \langle c_{i \gamma} \rangle^\gamma = 0 \quad (5)$$

In addition, since the β phase is multiply connected and homogeneous (each cell has uniform ion concentrations), the transport terms intrinsic to β phase are zero. The evolution of the properties of the β phase (volume fraction and ion concentration) with time is described by the cell model described below. Equation (2) can be integrated to yield the local concentrations of ion i in each phase, given the molecular velocity \mathbf{v}^* . A number of simplifications can be made. The assumption of zero bulk motion through the layer implies that the molar velocity is zero: $\mathbf{v}^*=0$. As Fig. 1 shows, the coordinate axes y and x are fixed parallel and perpendicular (outwards) to the skin surface, respectively. Given the histology of the epidermis, it is reasonable to assume that this coordinate system corresponds to the principal directions as far as mass transport is concerned. We then identify these axes with the principal directions of the effective total transport coefficient tensor (which includes molar diffusion and dispersion), with diagonal values D_{11}^{**} in x direction and D_{22}^{**} in y direction. The molecular velocity vector has components v_x and v_y . On the basis of the above simplifications we can rewrite Eq.(2), in less compact form. Equation (6) below expresses the transient behavior of the ion concentrations in phase α as affected by diffusion and volume fraction variation. The β phase changes volume and absorbs or eliminates solutes, acting as sink/source according to extracellular concentrations, as better explained on the next section.

$$\begin{aligned} \theta_\alpha \frac{\partial \langle c_{i \alpha} \rangle^\alpha}{\partial t} &= \theta_\alpha D_{11}^{**} \frac{\partial^2 \langle c_{i \alpha} \rangle^\alpha}{\partial x^2} + \left(D_{11}^{**} \frac{\partial \theta_\alpha}{\partial x} + \theta_\alpha \frac{\partial D_{11}^{**}}{\partial x} - \theta_\alpha v_{x \alpha} \right) \frac{\partial \langle c_{i \alpha} \rangle^\alpha}{\partial x} + \\ &\theta_\alpha D_{22}^{**} \frac{\partial^2 \langle c_{i \alpha} \rangle^\alpha}{\partial y^2} + \left(D_{22}^{**} \frac{\partial \theta_\alpha}{\partial y} + \theta_\alpha \frac{\partial D_{22}^{**}}{\partial y} - \theta_\alpha v_{y \alpha} \right) \frac{\partial \langle c_{i \alpha} \rangle^\alpha}{\partial y} + \\ &\left(-\theta_\alpha \frac{\partial v_{x \alpha}}{\partial x} - \theta_\alpha \frac{\partial v_{y \alpha}}{\partial y} - v_{x \alpha} \frac{\partial \theta_\alpha}{\partial x} - v_{y \alpha} \frac{\partial \theta_\alpha}{\partial y} - \frac{\partial \theta_\alpha}{\partial t} \right) \langle c_{i \alpha} \rangle^\alpha + \\ &\left(-\frac{\partial \theta_\beta}{\partial t} \langle c_{i \beta} \rangle^\beta - \frac{\partial \langle c_{i \beta} \rangle^\beta}{\partial t} \theta_\beta \right) \end{aligned} \quad (6)$$

The above equation is coupled to Eq.(7) below, which is consistent with volume conservation in the mixture α , β , γ , and Eq.(4).

$$\frac{\partial \theta_\alpha}{\partial t} = -\frac{\partial \theta_\beta}{\partial t} \quad (7)$$

2.2. Single Cell Model

The animal cell volume is directly associated with the water transport across the membrane, which is regulated by osmotic gradient, cf. Boron and Boulpaep, 2003. Any osmotic imbalance between the extracellular and intracellular space is corrected by water transport (via aquaporins, Reuss and Hirst, 2002) and ion exchange (via specialized ion channels or ion pumps) across the cell membrane. Potassium, chloride and sodium ions are

the relevant ions in terms of volume regulation, and most of them are free in solution (and therefore free to diffuse) in both intracellular and extracellular compartments. Each ion passively crosses the membrane through ion channels down its electrochemical gradient. In order to maintain intracellular concentrations high for K^+ and low for Na^+ , the sodium-potassium pump ($Na^+ - K^+ - ATPase$) uses energy from ATP oxidation to transport ions against the electrochemical gradient. Cotransporters translocate two (or more) solutes in the same direction according to the stronger electrochemical gradient among its components, carrying the other ions against their gradient passively. The cell volume regulation scheme developed by Hernandez and Cristina, 1998, and adopted here is briefly presented below for completeness. Five assumptions are made to describe the animal cell represented by the model: (a) non-polarized cells; (b) cell volume changes caused by water movement across the membrane; (c) fixed stoichiometric pump ratio of $3Na^+ : 2K^+$; (d) the cell volume decrease is mediated by coupled flux of K^+ and Cl^- , and the increase by Na^+ and Cl^- flux. Two volume thresholds v^+ and v^- are considered, in terms of activating a net KCl efflux or NaCl influx; (e) constant cell surface area A_c for water transport.

The electrodiffusive fluxes J_i and the cycle flux J_p (a consequence of intracellular electroneutrality condition) through the cell membrane is given by:

$$J_K = P_K \frac{\frac{F V_m}{R T}}{e^{\frac{F V_m}{2 R T}} - e^{-\frac{F V_m}{2 R T}}} \left(\langle c_{K \alpha} \rangle^\alpha e^{-\frac{F V_m}{2 R T}} - \frac{m_K}{V_c} e^{\frac{F V_m}{2 R T}} \right) \quad (8)$$

$$J_{Na} = P_{Na} \frac{\frac{F V_m}{R T}}{e^{\frac{F V_m}{2 R T}} - e^{-\frac{F V_m}{2 R T}}} \left(\langle c_{Na \alpha} \rangle^\alpha e^{-\frac{F V_m}{2 R T}} - \frac{m_{Na}}{V_c} e^{\frac{F V_m}{2 R T}} \right) \quad (9)$$

$$J_{Cl} = P_{Cl} \frac{\frac{F V_m}{R T}}{e^{\frac{F V_m}{2 R T}} - e^{-\frac{F V_m}{2 R T}}} \left(\langle c_{Cl \alpha} \rangle^\alpha e^{\frac{F V_m}{2 R T}} - \frac{m_{Cl}}{V_c} e^{-\frac{F V_m}{2 R T}} \right) \quad (10)$$

$$-J_p + J_{Na} + J_K - J_{Cl} = 0 \quad (11)$$

where m_i is the intracellular molar concentration of ion i , P_i is the membrane permeability coefficient, V_c represents the cell volume, V_m the intracellular potential minus the extracellular potential, F is Faraday constant (current = $F \times$ ion flux), R is the ideal gas constant, and T the absolute temperature.

The ion concentrations and cell volume are governed by the following ODEs:

$$\frac{dm_{Na}}{dt} = A_c (-3 J_p + J_{Na} + \phi_{Na}) \quad (12)$$

$$\frac{dm_K}{dt} = A_c (2 J_p + J_K + \phi_K) \quad (13)$$

$$\frac{dm_{Cl}}{dt} = A_c (J_{Cl} + \phi_{Na} + \phi_K) \quad (14)$$

$$\frac{dV_c}{dt} = (A_c V_w P_w) \left(\frac{(m_X + m_{Na} + m_K + m_{Cl})}{V_c} - (\langle c_{X \alpha} \rangle^\alpha + \langle c_{Na \alpha} \rangle^\alpha + \langle c_{K \alpha} \rangle^\alpha + \langle c_{Cl \alpha} \rangle^\alpha) \right) \quad (15)$$

with V_w as the partial molar volume of water, P_w the osmotic permeability, X the non-permeant solute, $\langle c_{i \alpha} \rangle^\alpha$ the extracellular solute concentration under isotonic conditions, and $\phi_{Na, K}$ are the volume-induced fluxes of NaCl and KCl. The membrane potential is related to the various cell parameters through the following algebraic equation:

$$V_m = \frac{RT}{F} \ln \left(\frac{\kappa + \lambda}{\mu + \omega} \right) \quad (16)$$

The terms in the logarithm represent functions of intracellular and extracellular concentrations, membrane permeabilities, $Na^+ - K^+ - ATPase$ membrane density, and the rate constants associated with the transmembrane pumps.

While $v^- < V_c < v^+$ is satisfied, the induced fluxes ϕ_{Na} and ϕ_K are null. Whenever the cell volume exceeds the acceptable threshold value, and after a predetermined time delay τ , an appropriate volume-induced flux (ϕ_{Na} for $V_c < v^-$ and ϕ_K for $V_c > v^+$) is initiated and is set to the values given by Eq.(17) or Eq.(18) below, in order to restore the cell to its physiological parameters:

$$\phi_{Na} = Q_{Na}^* \frac{(v^- - V_c)}{v^-} \left(\langle c_{Na \alpha} \rangle^\alpha \langle c_{Cl \alpha} \rangle^\alpha - \frac{m_{Na} m_{Cl}}{V_c^2} \right) \quad (17)$$

$$\phi_K = Q_K^* \frac{(V_c - v^+)}{v^+} \left(\langle c_{K \alpha} \rangle^\alpha \langle c_{Cl \alpha} \rangle^\alpha - \frac{m_K m_{Cl}}{V_c^2} \right) \quad (18)$$

2.3. Physicochemical and Numerical Parameters

The living epidermis has a thickness between 30 to 130 μm , and features the highest water content in the skin, ranging from more than 70% (in the basement membrane) to 15% (top of the stratum corneum layer). We consider a stratified medium confined in a homogeneous layer and limit the model to transport in two dimensions, x (perpendicular to layer) and y (parallel to the layer), as shown in Figure 1. For definitiveness, we consider here an epidermal layer thickness of 100 μm and use as initial condition $\theta_\alpha = 0.2$, $\theta_\beta = 0.4$ and $\theta_\gamma = 0.4$. Many of the transport parameters of the intracellular model are adopted directly from Hernandez and Cristina, 1998, with a delay of $\tau = 10$ sec, and a volume change threshold of 5%. We finally need to prescribe the variation of the extracellular dispersion coefficient with the volume fraction of phase α . Assuming a homogeneous "brick and mortar" wall-like distribution of keratinocytes, the following expression for the ratio $\lambda^2 = D_{mi}/D^{**}$ is obtained by manipulating the results obtained by Chen and Nicholson, 2000:

$$\lambda = 2.28156 - 5.21948 \theta_\alpha + 15.6529 \theta_\alpha^2 - 19.1835 \theta_\alpha^3 + 7.46849 \theta_\alpha^4 \quad (19)$$

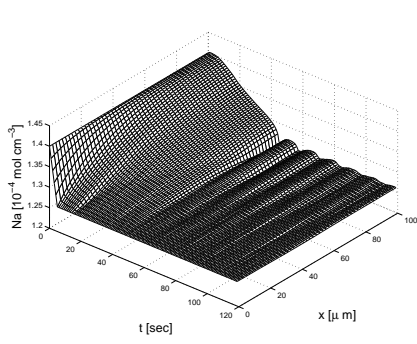
The initial condition is defined by prescribing uniform concentrations of all ions across the layer with all cells at identical state and at equilibrium. At time $t > 0$, the Na^+ and Cl^- extracellular concentrations at the basal surface ($x = 0$) are lowered by 10% (increased by 10%) by ramping to the final value within 5 sec. This corresponds to exposing the epidermis to a hyposmotic (hyperosmotic) shock as a result of supplying plasma of diminished (increased) salinity at the basal membrane level. The above set of parameters, including all ion equilibrium concentrations which are identical with Hernandez and Cristina, 1998, constitute the control state, which will be varied in order to examine the cell response characteristics in the following systematic study.

Assuming periodic conditions along the surface of the skin (y direction), the physical problem becomes essentially one-dimensional. Applying Eq.(6) for the four species, supplemented by the four cell equations (12-15), produce a system of 8 evolution equations with 8 unknowns (4 in phase α and 4 in β). Using finite-difference discretization, the equations are integrated in time with the ADI scheme for the extracellular equations and a 4th order Runge-Kutta scheme for the cell ODE's. The time step was set at 10^{-3} seconds and a uniform mesh with 50 nodes was used in the x direction.

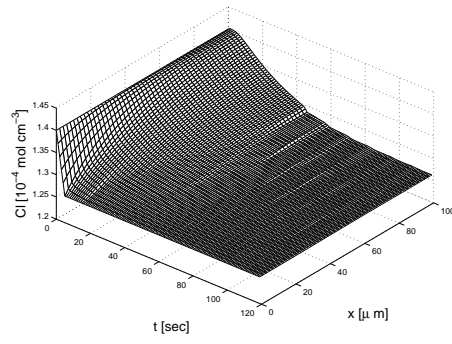
3. Results

The results obtained with the control physicochemical parameters are presented in Fig. 2 and can be organized in two groups: Figs. 2(a-f) correspond to the hyposmotic and Figs. 2(e-h) to the hyperosmotic shocks. Fig. 2(c) depicts the variation of the volume fraction α , which is the extracellular fluid phase, for hyposmotic shock, while Fig. 2(g) corresponds to the hyperosmotic shock. One can readily observe that the presence of the cell phase is associated with the appearance of an undershoot (overshoot) which corresponds to a transient swelling (shrinking) of the cells in response to the initial shock. Only in the case of the hyposmotic shock is the initial undershoot followed by a series of propagating waves starting from the basal side of the layer ($x = 0 \mu\text{m}$) where the shock is imposed. We hypothesize that these waves are caused by the delayed activation of the cell membrane cotransporters introduced in the model of Hernandez and Cristina, 1998, in conjunction with the high value of the volume-induced flux in Eq.(15). Our hypothesis related to the latter condition is motivated by the observation that the amplitude of the volume-induced flux of the K ion is much larger than that for the Na ion by two magnitudes of order ($Q_K^* \gg Q_{Na}^*$). This will be tested below by varying Q_K^* . The wave period is approximately twice the $\tau = 10$ sec value, and this will be also explored further below. Fig. 2(d) shows the corresponding behavior of the extracellular Na and Fig. 2(f) the dramatic behavior of intracellular K for the hyposmotic shock. Indeed, the intracellular concentration of K exhibits a delayed 50% increase on the apical side of the layer ($x = 100 \mu\text{m}$). The features of the hyperosmotic case (Figs. 2(e-h)) are unremarkable.

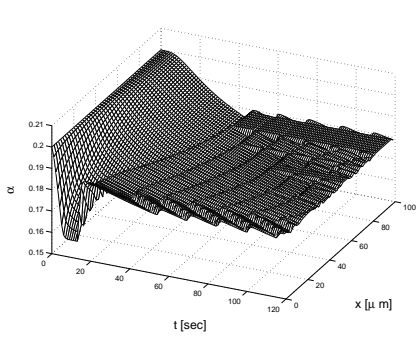
We have performed a further numerical study of the hyposmotic case by changing two of the parameters in a systematic way: τ and Q_K^* . The results in terms of the variation of the volume fraction α are plotted in Fig. 3. The data of Figs. 3(a, b) are identical with only a slight change of perspective. Figs. 3(a, c, e) show the effect of decreasing the time delay before the volume-induced flux is activated. As τ diminishes to zero, the travelling waves that are generated near the basal side of the layer diminish in amplitude and period. This phenomenon is consistent with the role that the time delay plays in restoring the cell properties near the threshold values. The system of equations (12- 15) coupled with Eq.(6) represent a dynamic system with an equilibrium point which is set by the threshold values. As the cell volume swells in response to the hyposmotic shock, the K-flux given by Eq.(18) does not come into play until a time period equal to τ . The shorter this period is, the shorter the period of oscillation around the equilibrium point, and the lower the undershoot and the subsequent imbalances of the cell with its extracellular space. Figs. 3(b, d, f) show the effect of decreasing the value of Q_K^* with τ fixed. Decreasing this value by half the control value shown in Fig. 3(a), limits the travelling wave to a smaller spatial domain and causes damping in time (Fig. 3(b)). A decrease of one magnitude of order eliminates the travelling



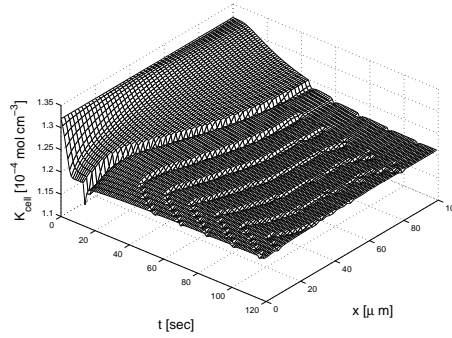
(a) Hyposmotic, extracellular Na



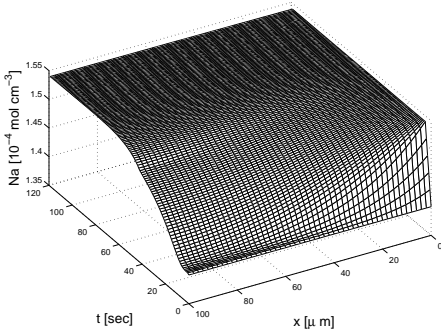
(b) Hyposmotic, extracellular Cl



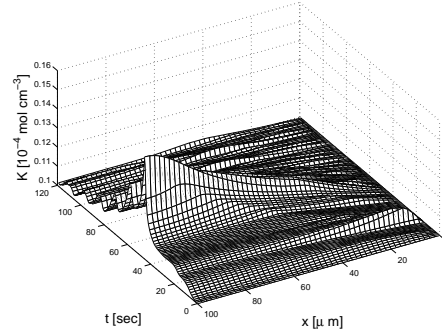
(c) Hyposmotic, α



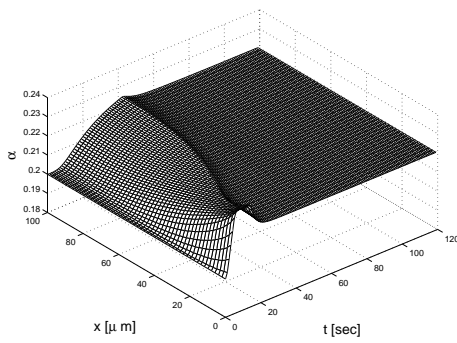
(d) Hyposmotic, intracellular K



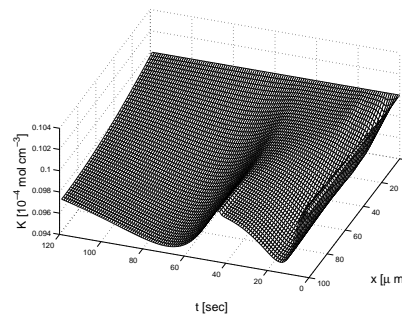
(e) Hyperosmotic, extracellular Na



(f) Hyperosmotic, extracellular K



(g) Hyperosmotic, α



(h) Hyperosmotic, extracellular K

Figure 2: Effects of 10% hyposmotic and hyperosmotic shock in both Na^+ and Cl^- concentrations.

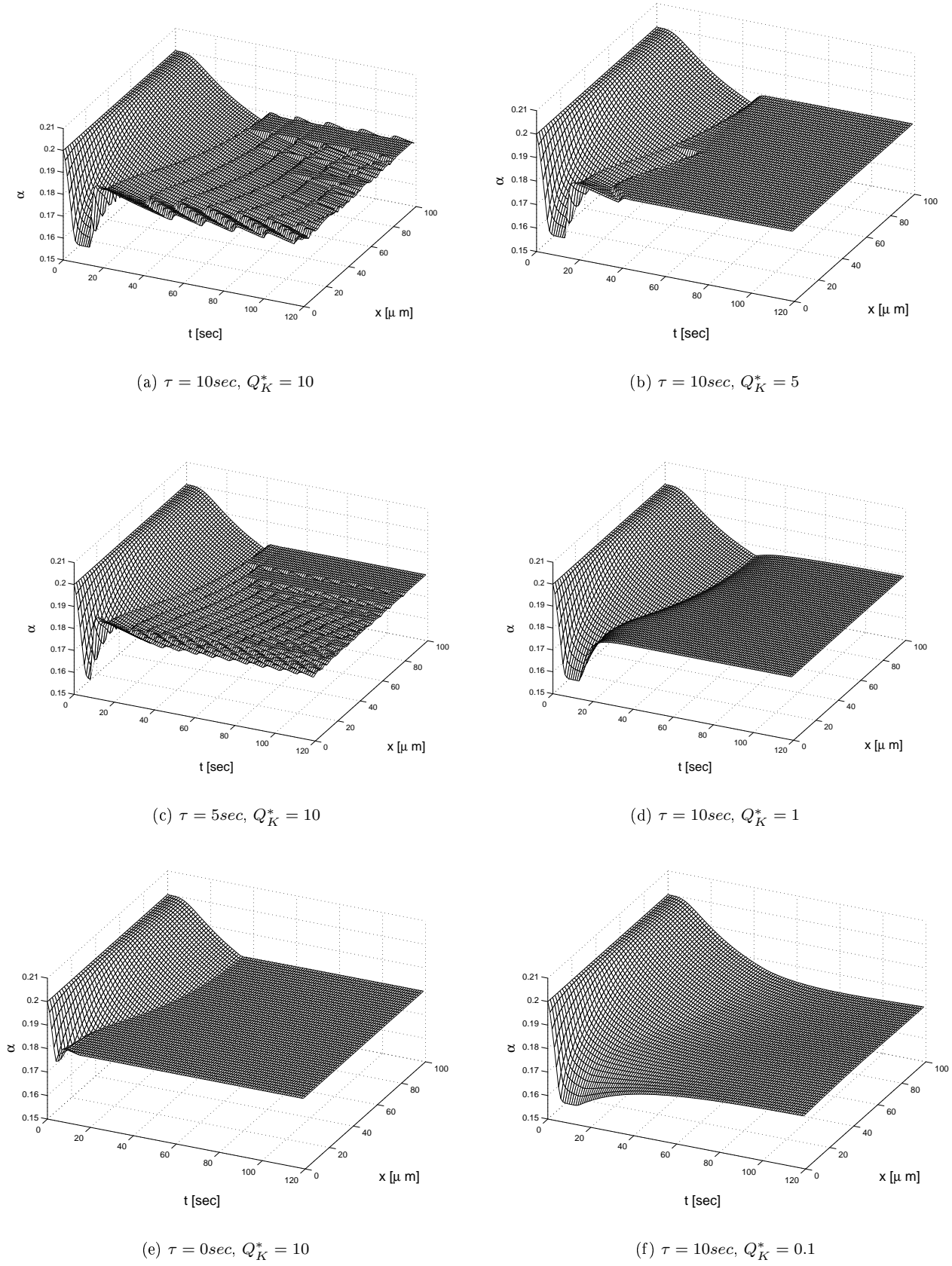


Figure 3: Effects of τ and Q_K^* on α in hypersonic shocks.

waves (Fig. 3(d)), while decreasing the value by 100 results in a smoother response recover to the shock (Fig. 3(f)). This indicates that decreasing the intensity of the volume-induced KCl cotransporter (expressed by Q_K^* value) increases the damping constant of the corresponding dynamic system.

Although not shown here, the numerical results we obtained for the case of $\beta = 0$ (no cells) reveal no travelling waves as a response of an osmotic shock in the layer. This is expected since the extracellular transport is purely diffusive in the absence of cells which act like sources/sinks with time delay. It is therefore clear that the travelling waves are a result of the restorative effect of the cell phase and a consequence of transcellular active transport. A careful review of the literature has not revealed another report of this phenomenon. The onset of dispersive (wave-like) behavior in systems that are typically modelled by diffusive partial differential equations has an obvious mathematical appeal. If shown to be realistic, the generation of travelling waves in live tissue consisting of non-excitabile cells might prove to serve an important physiological function which is as fascinating as that exhibited by excitable cells (neurons).

4. Conclusions

This is a numerical study of the redistribution of both extracellular (interstitial) and intracellular water and active mass transport through epidermal cells (keratinocytes) in the viable epidermis exposed to osmotic shocks imposed on its basal side. We model the redistribution of water coupled to ion transport in a coarse-grained model of the skin consisting of free interstitial water, live cells, and inert extracellular matrix (triphase medium). The volume of the cell phase depends on the fluxes of water and Na^+ , K^+ and Cl^- ions across the cell membrane and is regulated according to the model of Hernandez and Cristina, 1998. A parametric numerical simulation study of the response of the active triphasic medium exposed to osmotic shocks at one boundary reveals novel travelling waves in the case of hyposmotic shocks. The amplitude and strength of these travelling waves depend on time delay and the magnitude the volume-induced ion flux involved in the activation of the cells when certain threshold values are exceeded. The present work reports the first -to our knowledge- local model for the viable epidermis which couples active transport of water and electrolyte transport through the membrane of the epidermal cells (keratinocytes) and the extracellular matrix.

5. Acknowledgements

The authors appreciate the support of the Coordenação de Aperfeiçoamento de Pessoal del Nível Superior (CAPES - Brazil) in the form of a graduate fellowship for C.V.F. and of the USA National Science Foundation through the Science and Technology Center of Advanced Materials for the Purification of Water with Systems (CAMPWS, cooperative agreement CTS-0120978). The authors would also like to thank John Selby for many fruitful discussions regarding the histology and function of the epidermis.

6. References

- Bear, J. and Buchlin, J.-M., 1987, "Modelling and Applications of Transport Phenomena in Porous Media", Kluwer Academic Publishers, Netherlands.
- Boron, W. F. and Boulpaep, E. L., 2003, "Medical Physiology", Saunders, China.
- Chen, K. C. and Nicholson, C., 2000, Changes in Brain Cell Shape Create Residual Extracellular Space Volume and Explain Tortuosity Behavior During Osmotic Challenge, "Proceedings of the National Academy of Sciences of the United States of America", Vol. 97, pp. 8306–8311.
- Chinard, F. P., 2000, Solute Exchanges. How Far Have We Come in 100 Years? What's Next?, "Annals Of Biomedical Engineering", Vol. 28, pp. 849–859.
- Falkenberg, C. V. and Georgiadis, J. G., 2004, Water and Solute Active Transport through Model Epidermis: Contribution of Electrodiffusion, "Proceedings of ASME International Mechanical Engineering Conference", Anaheim, CA, U.S.A.
- Freinkel, R. K. and Woodley, D. T., 2001, "The Biology of The Skin", The Parthenon Publishing Group, New York, USA.
- Gu, W. Y., Lai, W. M., and Mow, V. C., 1998, A Mixture Theory for Charged-Hydrated Soft Tissues Containing Multi-electrolytes: Passive Transport and Swelling Behaviors, "ASME Journal of Biomechanical Engineering", Vol. 120, pp. 169–180.
- Gu, W. Y., Lai, W. M., and Mow, V. C., 1999, Transport of Multi-electrolytes in Charged Hydrated Biological Soft Tissues, "Transport in Porous Media", Vol. 34, pp. 143–157.
- Hernandez, J. A. and Cristina, E., 1998, Modeling Cell Volume Regulation In Nonexcitable Cells: the Roles of the Na^+ pump and of Cotransport Systems, "American Journal of Physiology", Vol. 275, pp. C1067–C1080.
- Reuss, L. and Hirst, B. H., 2002, Water Transport Controversies - an overview, "Journal of Physiology", Vol. 542, pp. 1–2.

Verkman, A. S., 2000, Water Permeability Measurement in Living Cells and Complex Tissues, “Journal of Membrane Biology”, Vol. 173, pp. 73–87.